Energy & Environmental Science

Cite this: *Energy Environ. Sci.*, 2012, **5**, 7531

www.rsc.org/ees

COMMUNICATION

Metal hydrazinoborane $LiN_2H_3BH_3$ and $LiN_2H_3BH_3 \cdot 2N_2H_4BH_3$: crystal structures and high-extent dehydrogenation†

Hui Wu,*[ab] Wei Zhou,[ab] Frederick E. Pinkerton,[c] Terrence J. Udovic,[a] Taner Yildirim[ad] and John J. Rush[ab]

Received 28th February 2012, Accepted 30th March 2012
DOI: 10.1039/c2ee21508j

The first example of metal hydrazinoborane, $LiN_2H_3BH_3$, and its hydrazine borane adduct $LiN_2H_3BH_3 \cdot 2N_2H_4BH_3$ were synthesized with their crystal structures successfully determined. The metal hydrazinoboranes exhibit dramatically improved dehydrogenation over the pristine hydrazine borane ($N_2H_4BH_3$) with nearly complete dehydrogenation in a mild temperature range (50–225 °C) and high purity of H_2 release.

Hydrogen in combination with a fuel cell is the most attractive option for a long-term sustainable energy development. One of the most critical factors in realizing a hydrogen economy is finding an efficient hydrogen storage material. Among a variety of developed hydrogen storage materials, ammonia borane (NH_3BH_3, AB) has attracted broad attention owing to its high gravimetric capacity of H_2 (19.6 mass%). Many approaches have been developed to promote its hydrogen release.[1–6] Particularly, one the most important breakthroughs for ammonia borane to be used for automobile applications is the discovery of its regeneration from the main component in spent fuel (polyborazylene, PB) by direct reaction with hydrazine and liquid ammonia.[7] It was also found that PB reacts with hydrazine in THF solution to form hydrazine borane ($N_2H_4BH_3$, HB). This fact that HB can be generated from the spent fuel of AB makes it a closely related compound to AB as a potential hydrogen storage material and therefore HB based materials deserve further investigations.

HB, with a high hydrogen content (15.4 mass%), also contains both hydridic and protic hydrogens, which will facilitate hydrogen release under mild conditions. The thermal decomposition of pure HB was first studied five decades ago.[8] Pure HB melts at 61 °C, at which point decomposition slowly starts and yields $(NHBH_2)_2$, toxic hydrazine (N_2H_4), ammonia (NH_3) and H_2 after pyrolysis.[8,9] Hydrolysis of HB without a catalyst also leads to the concurrence of free N_2H_4.[10] Unlike the NH_3 group of AB, the N_2H_4 group of HB can also be dehydrogenated in the presence of a selective catalyst, although this reaction competes with NH_3 release. Thus efforts have been made to produce complete dehydrogenation of HB, mostly *via* catalyst-assisted hydrolysis.[10,11] Significant improvement in the thermolysis dehydrogenation was recently observed in HB–LiH mixtures in terms of accelerated decomposition kinetics and reduced foaming issues.[12] However, the lack of identification of the products before and after dehydrogenation of HB–LiH mixtures makes a subsequent dehydrogenation mechanism study and regeneration investigation

[a]*NIST Center for Neutron Research, National Institute of Standards and Technology, Gaithersburg, MD 20899-6102, USA. E-mail: huiwu@nist.gov*
[b]*Department of Materials Science and Engineering, University of Maryland, College Park, MD 20742-2115, USA*
[c]*Chemical Sciences and Materials Systems Laboratory, General Motors Research and Development Center, Warren, MI 48090-9055, USA*
[d]*Department of Materials Science and Engineering, University of Pennsylvania, Philadelphia, PA 19104-6272, USA*

† Electronic supplementary information (ESI) available: Experimental section; crystallographic data of $LiN_2H_3BH_3$, $LiN_2H_3BH_3 \cdot 2N_2H_4BH_3$ and $N_2H_4BH_3$; XRD patterns; and hydrogen release rate/kinetics study. See DOI: 10.1039/c2ee21508j

Broader context

One of the major challenges to the widespread use of hydrogen as a primary fuel is the lack of suitable hydrogen storage materials with the on-board operating storage capabilities for fuel-cell vehicular applications. Tremendous efforts have been recently made on the light-weight B–N–H complex–chemical hydride systems mostly due to the coexistence of hydridic ($H^{\delta-}$) and protic ($H^{\delta+}$) hydrogen therein, which has been proved to effectively facilitate hydrogen release from these materials. Hydrazine borane ($N_2H_4BH_3$, HB), with a high hydrogen content (15.4 mass%), has attracted great attention as a promising hydrogen storage material. However, H_2 release from HB during thermolysis is slow and is contaminated with significant toxic hydrazine (N_2H_4). Herein, we report the discovery and crystal structure determination of the first metal hydrazinoboranes, $LiN_2H_3BH_3$ and $LiN_2H_3BH_3 \cdot 2N_2H_4BH_3$, which possess novel structures, thanks to the bidentate nature of the hydrazinoborane $[N_2H_3BH_3]^-$ ligand. These metal hydrazinoboranes exhibit high extent of dehydrogenation with better kinetics and minimal unwanted byproduct gases compared to the pristine HB. $LiN_2H_3BH_3$ and $LiN_2H_3BH_3 \cdot 2N_2H_4BH_3$ are the first two examples of a potentially large class of new B/N-containing hydrogenous compounds for hydrogen storage.

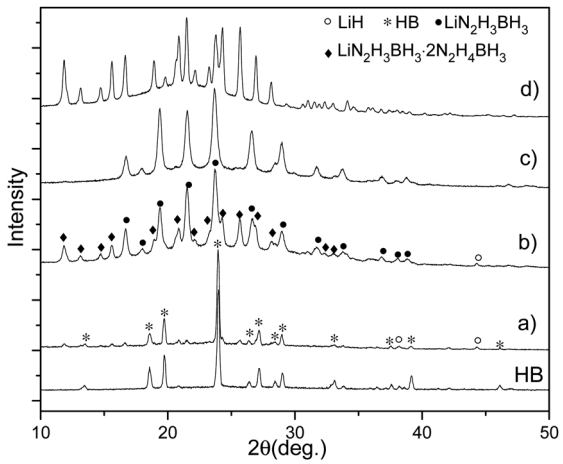

Fig. 1 XRD patterns of the bare HB (bottom) and (a) hand-mixed 1 : 1 HB–LiH in a mortar; (b) ball-milled 1 : 1 HB–LiH for 1 h; (c) single-phase $LiN_2H_3BH_3$ after ball-milling 1 : 1 HB–LiH for 3 h; (d) single-phase $LiN_2H_3BH_3{\cdot}2N_2H_3BH_3$ after ball-milling 3 : 1 HB–LiH for 1 h.

difficult. Therefore, it is of great interest to better understand the structures and identities of the compounds in HB–LiH mixtures, which is also crucial for further rational experimental and theoretical investigation in the HB-derived materials. Herein, we report the discovery and crystal structure determination of the first metal hydrazinoboranes, $LiN_2H_3BH_3$ and $LiN_2H_3BH_3{\cdot}2N_2H_4BH_3$, which possess novel structures, thanks to the bidentate nature of hydrazinoborane ligand. These metal hydrazinoboranes exhibit high extent dehydrogenation with better kinetics and minimal unwanted byproduct gases compared to the pristine HB.

Even though Lentz *et al.*[12] have reported the dehydrogenation properties of a 1 : 1 ratio of HB and LiH mixture, the nature of this mixture has not been determined. Our study indicated that such hand-mixed powders are mainly a mixture of HB and LiH phases (Fig. 1a). The X-ray diffraction (XRD) peaks from HB and LiH disappeared only after ball-milling a 1 : 1 HB–LiH mixture for 1 h (Fig. 1b). However, this pattern could not be indexed as a single phase. Extended ball-milling finally resulted in a single-phase XRD pattern (Fig. 1c), which could be indexed using a monoclinic $P2_1/c$ unit cell with $a = 5.8521$ Å, $b = 7.4655$ Å, $c = 8.8973$ Å, and $\beta = 122.381°$ (compound I). With increasing HB to LiH ratio, peaks from this phase gradually weakened, while another set of peaks became prominent. Finally, for a 3 : 1 HB–LiH mixture after ball-milling, all the peaks could be indexed to a $P2_1/c$ monoclinic single phase with $a = 8.1495$ Å, $b = 8.9605$ Å, $c = 14.9720$ Å, and $\beta = 116.091°$ (Fig. 1d, compound II). Rechecking the 1 : 1 HB–LiH XRD spectra measured after hand-mixing or short milling time (Fig. 1a and b), it was found that this pattern actually contained both compounds I and II, indicating an incomplete reaction between HB and LiH.

The crystal structures of I and II were then solved using combined direct methods and first-principles molecular dynamics simulated annealing, which revealed compounds of lithium hydrazinoborane and its hydrazine borane adduct with stoichiometries of $LiN_2H_3BH_3$ (I) and $LiN_2H_3BH_3{\cdot}2N_2H_4BH_3$ (II), respectively. It can be seen from inspection of the Rietveld fits to the XRD patterns that all the reflections of $LiN_2H_3BH_3$ and $LiN_2H_3BH_3{\cdot}2N_2H_4BH_3$ can be fit very well using the determined structure models (Fig. S1 and S2, ESI†), which strongly supports the validity of our structure solutions. Note that the refinement based on laboratory X-ray data cannot provide highly accurate atomic coordinates, especially for H. First-principles calculations were thus performed, and the fully relaxed structure is used in the bond length discussion below.

Fig. 2 shows the derived crystal structures for $LiN_2H_3BH_3$ and $LiN_2H_3BH_3{\cdot}2N_2H_4BH_3$. In $LiN_2H_3BH_3$, it can be seen that during the reactions between HB and LiH, the strong Lewis base H^- in LiH deprotonates the H^+ on the middle N (N1) while the Hs on the terminal N (N2) remain unperturbed. Li^+ then combines with the $NH_2NHBH_3^-$ ion and forms $NH_2NHLiBH_3$. The middle N retains its tetrahedral sp^3 hybridization with one H replaced by Li^+ and a Li–N distance of 2.105 Å. The Li^+ also interacts with the lone pair electrons of the terminal N in another $NH_2NHBH_3^-$ ion with a Li–N distance of 2.124 Å, and coordinates with two other BH_3 units in the neighboring $NH_2NHBH_3^-$ ions, constructing a tetrahedral coordination (Fig. 2a and b). Note that further increasing LiH (*i.e.*, an increased LiH–HB ratio >1 : 1) did not lead to the removal of more Hs from HB, but rather resulted only in a mixture of extra LiH and $LiN_2H_3BH_3$ with poor crystallinity.

In $Li(N_2H_3BH_3){\cdot}2N_2H_4BH_3$, the Li replaces one H on the internal N of one HB molecule and forms $NH_2NHLiBH_3$ as a result of the reaction between H^+ and the H^- from LiH. This Li^+ ion also directly interacts with the lone-pair electrons of the terminal N of the second $NH_2NHLiBH_3$. Likewise, the Li in the second $NH_2NHLiBH$ bonds equally with the terminal N of the first $NH_2NHLiBH$ *via* its lone pair electrons (Fig. 2d). Besides the $NH_2NHBH_3^-$ ions, these Li^+ ions also bond to the terminal Ns of the other two undeprotonated HB molecules, respectively. The two $NH_2NHBH_3^-$ ions in fact serve as bridges connecting this pair of $Li[N_2H_3BH_3]_2[N_2H_4BH_3]_2$ tetrahedra, leading to the formation of a $Li_2[N_2H_3BH_3]_2[N_2H_4BH_3]_4$ complex pair (Fig. 2d). The distances from Li^+ to the Ns in $NH_2NHBH_3^-$ or $N_2H_4BH_3$ are shown in Fig. 2d. In contrast to the ionic structure $LiN_2H_3BH_3$, where Li^+ interacts with $NH_2NHBH_3^-$ on each internal and terminal N and BH_3 throughout the whole crystal structure,

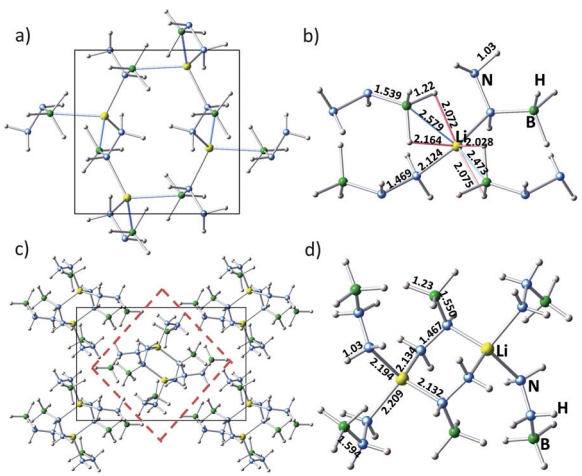

Fig. 2 Crystal structures and Li coordination environments of $LiN_2H_3BH_3$ (a and b) and $LiN_2H_3BH_3{\cdot}2N_2H_4BH_3$ (c and d). In $LiN_2H_3BH_3$, Li is tetrahedrally coordinated with four $N_2H_3BH_3^-$ ions through one internal N, one terminal N, and two BH_3 of each $LiN_2H_3BH_3$. In $LiN_2H_3BH_3{\cdot}2N_2H_4BH_3$, Li tetrahedrally bonds with N only (one internal N and three terminal N), forming a $Li_2[N_2H_3BH_3]_2[N_2H_4BH_3]_4$ molecular cluster. $LiN_2H_3BH_3{\cdot}2N_2H_4BH_3$ is built from such clusters highlighted within the red dashed box.

$LiN_2H_3BH_3 \cdot 2N_2H_4BH_3$ is actually built of $Li_2[N_2H_3BH_3]_2$-$[N_2H_4BH_3]_4$ molecular clusters (Fig. 2c), which are independent and only in contact with each other through molecular bonding. Hence, $Li(N_2H_3BH_3) \cdot 2N_2H_4BH_3$ is essentially a molecular compound.

Compared to the bare HB structure, the B–N and N–N bond distances of $N_2H_3BH_3^-$ in $LiN_2H_3BH_3$ and $LiN_2H_3BH_3 \cdot 2N_2H_4BH_3$ are noticeably changed due to the deprotonation and the interaction with Li^+. The B–N bonds are significantly shortened from 1.596 Å (in HB) to 1.550 Å (in $Li(N_2H_3BH_3) \cdot 2N_2H_4BH_3$) and to 1.539 Å (in $LiN_2H_3BH_3$), whereas the N–N distances are stretched from 1.452 Å (in HB) to 1.467 Å (in $LiN_2H_3BH_3 \cdot 2N_2H_4BH_3$) and 1.469 Å (in $LiN_2H_3BH_3$). While for the HB molecules in $Li(N_2H_3BH_3) \cdot 2N_2H_4BH_3$, the B–N distances are little changed (1.59 Å and 1.60 Å) compared to the bare HB, the N–N bonds are indeed lengthened (*i.e.* 1.460 Å and 1.466 Å). The compressed B–N bonds in $N_2H_3BH_3^-$ clearly result from the stronger electron donation from Li toward N than from H. The same trend in changing B–N distances was also observed in AB and metal amidoboranes (MABs).[13] On the other hand, the lengthened N–N distances should be mainly the consequence of the interactions between Li^+ and the lone-pair electrons of the terminal N.

Similar to other B–N containing hydrogenous compounds, it is interesting to more closely inspect the extent of the dihydrogen bonding in $LiN_2H_3BH_3$ and $Li(N_2H_3BH_3) \cdot 2N_2H_4BH_3$. As mentioned above, $LiN_2H_3BH_3$ is an ionic compound, while the crystal structure shows that all Hs on N have short separations, in a range of 2.003 Å to 2.102 Å, to their neighboring Hs on B, which indicates a rather strong dihydrogen bonding present in the structure as well (Fig. S4†). For the molecular $LiN_2H_3BH_3 \cdot 2N_2H_4BH_3$, the NH···HB distances between the $Li_2[N_2H_3BH_3]_2[N_2H_4BH_3]_4$ clusters are 1.813–2.387 Å (Fig. S4†), revealing that the dihydrogen bonding is the primary intermolecular interaction responsible for the stabilization of this molecular compound. In both $LiN_2H_3BH_3$ and $LiN_2H_3BH_3 \cdot 2N_2H_4BH_3$, the closest NH···HB distances are shorter than that in pure HB (2.010 Å).[14] Finally it is worth mentioning that, different from AB or MABs,[13] the intramolecular NH···HB distances are 2.362 Å in $LiN_2H_3BH_3$, and 2.32 Å and 2.386 Å in $LiN_2H_3BH_3 \cdot 2N_2H_4BH_3$, implying that the dihydrogen bonding is even present within each HB molecule and $NH_2NHBH_3^-$ ion.

Volumetric temperature programmed desorption (TPD) and the independent thermogravimetry analysis/mass spectroscopy (TG/MS) measurements were performed on $LiN_2H_3BH_3$ and $LiN_2H_3BH_3 \cdot 2N_2H_4BH_3$ to study their dehydrogenation properties (Fig. 3 and 4). TPD was also conducted on the pure HB for comparison. Pure HB releases only ~1.0 H_2 equiv. per mol HB between 100 and 150 °C, which is consistent with the previous observation, as the melt of HB forms upon decomposition and solidifies quickly above 150 °C.[12] $LiN_2H_3BH_3$ starts to release H_2 below 70 °C. Both TPD and TGA indicated two sharp gas release events between 100 and 200 °C with ~3H_2 equiv. per mol LiHB. TGA/MS showed that the main weight loss in this temperature range is predominantly H_2 (9.5 wt%, 92% of the total weight loss). H_2 is accompanied by a minor amount of N_2, especially at the second peak at 150 °C (0.7 mass%), and a very small concurrent release of NH_3 (0.1 mass%). Thus the second peak is stronger in the TGA measurement than the volumetric TPD measurement. The purity of H_2 evolved from $LiN_2H_3BH_3$ is much higher than the pristine HB,[8,9] LiH–HB mixture[12] and the recently reported $LiBH_4 \cdot N_2H_4$.[15] Note that the H_2 released from $LiN_2H_3BH_3$ in the present study is less than

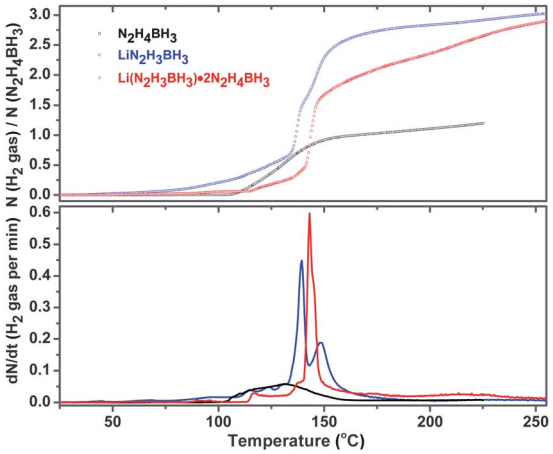

Fig. 3 TPD results of hydrogen release from HB, $LiN_2H_3BH_3$ and $LiN_2H_3BH_3 \cdot 2N_2H_4BH_3$ with 2 °C min^{-1} heating rate to 280 °C. The amount of H_2 gas released (top panel) has been normalized as n (H_2 gas) per mol $N_2H_4BH_3$. The hydrogen release rates are shown in the lower panel.

the reported HB–LiH mixture[12] because H_2 is lost during the ball-milling reaction of HB–LiH mixture (the theoretical H-content of is *ca.* 14.9 mass%) to form the $LiN_2H_3BH_3$ compound (*ca.* 11.7 mass %). The dehydrogenation of $LiN_2H_3BH_3 \cdot 2N_2H_4BH_3$ starts at

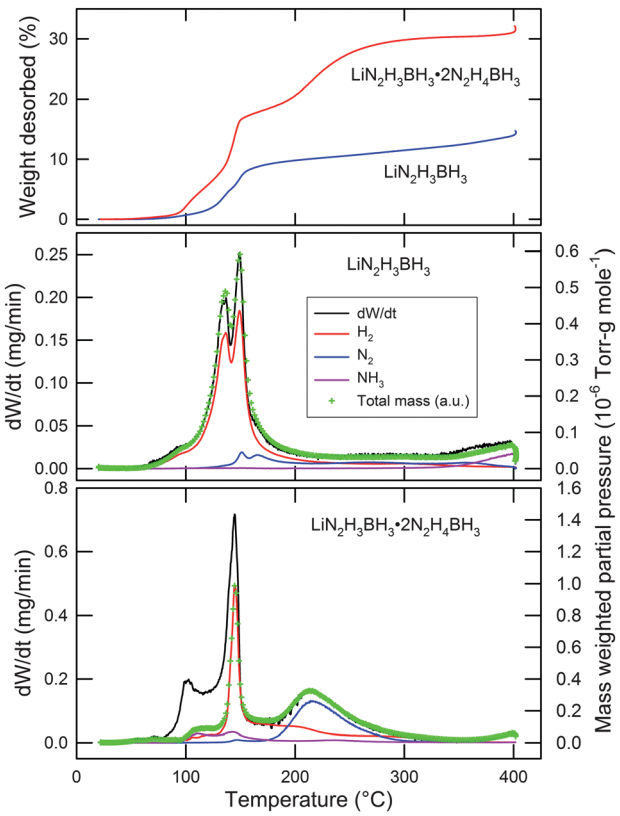

Fig. 4 TGA weight loss (upper panel) and the accompanying MS partial pressures (lower panel) for $LiN_2H_3BH_3$ and $LiN_2H_3BH_3 \cdot 2N_2H_4BH_3$ measured at 1.7 °C min^{-1} to 400 °C. The rate of mass loss dW/dt (black curve) is also shown. The green crosses are the total mass contribution to the evolved gas, scaled to compare with dW/dt.

~70 °C but is dominated by a single sharp main peak at 145 °C with a total 11.5 mass% H_2 release between 50 and 400 °C. An additional very small N_2 and NH_3 contribution is concurrent with H_2 at this temperature. More N_2 is released at the elevated temperature from 180 °C to 400 °C with a total of 8.9 mass%. Different from the well-behaved $LiN_2H_3BH_3$, there is insufficient gas detected at temperatures below 120 °C, as indicated by the discrepancy between the $dWl dt$ and the total MS mass shown by the green crosses in Fig. 4. No signatures were detected between 6 and 199 amu that could account for this mass loss, so it is certainly not diborane or borazine. It is likely that the sample emits a volatile heavy species (which was hardly detected in the volumetric TPD) above room temperature that recondenses prior to reaching the heated capillary tube to the mass spectrometer. This mass loss accounts for 9.0 mass% of the total mass loss (32.1 mass%), and is the preponderant mass loss below 120 °C. Detailed relative mass contributions to the total mass loss are listed in Tables S4 and S5†. Furthermore, consistent with the previous report on the LiH–HB mixtures and HB,[12] our kinetic studies indicated a dramatically accelerated hydrogen release rate of the HB–LiH mixtures compared to HB (Fig. S5†), *i.e.*, at 130 °C the HB–LiH mixtures release 7.9 mass% H_2 (~47% of its theoretical H amount) in 1 h, while HB only releases 4.8 mass% H_2 in 1 h. More interestingly, the hydrozinoborane $LiN_2H_3BH_3$ exhibits even better dehydrogenation rate and extent than the HB–LiH mixtures, *i.e.*, $LiN_2H_3BH_3$ releases 9.3 mass% H_2 (~80% of its theoretical H amount) under the same conditions described above. Therefore, the current systems, particularly $LiN_2H_3BH_3$, show remarkably improved dehydrogenation properties over pure HB at moderate temperatures. The net amount of hydrogen released and the NH_3 suppressed (*i.e.*, H_2 selectivity) from $LiN_2H_3BH_3$ far exceed the best performance reported for hydrolysis of HB with bimetallic nanocatalysts.[10]

Clearly the advantageous dehydrogenation properties of $LiN_2H_3BH_3$ and $LiN_2H_3BH_3 \cdot 2N_2H_4BH_3$ are not simply caused by the presence of the oppositely charged H, as the pure HB also contains both H^+ and H^-. It is more likely related to the formation of these new compounds with their unique crystal chemistry and the resulting changes in the nature and the reactivity of hydrogens, similar to that observed in the MABs.[13b] With replacement of Li for H on the middle N, more electrons are donated from the metal to $NH_2NHBH_3^-$ ions, and the hydridic nature of the B–H bond or the polarization of the B–H and B–N bonds is thus increased (Mulliken charges calculated in Table S6†), which enhances its reactivity compared to those in HB. Interestingly, even dative B–N bonds of the HB molecules in $LiN_2H_3BH_3 \cdot 2N_2H_4BH_3$ become polar compared to those in pristine HB (Table S6†). To confirm the effect of the active B–H bond on dehydrogenation, parallel experiments were conducted with addition of metal borohydride (MBH_4, M = Li, Na, Mg, and Ca) into HB. It was found that the active BH_4^- induced by MBH_4 could react with HB upon mixing, release gases, and form a transparent liquid or semi-transparent slurry. Note that MBH_4 does not deprotonate AB, but the mixtures either remain unreacted or form $MBH_4 \cdot AB$ complex adducts.[16] Apparently, the N_2H_4-terminal group and the polar B–N bond in HB and $N_2H_3BH_3^-$ are more sensitive to the active B–H than those in AB. The polar environments created by the charged $NH_2NHBH_3^-$ are expected to lower the reaction barrier and facilitate the intermolecular BH···HN interactions between the adjacent $[NH_2NHBH_3]^-$ ions compared to those between two neutral HB molecules in HB. The much more shortened BH···HN distances in the crystal structures of $LiN_2H_3BH_3$ and $LiN_2H_3BH_3 \cdot 2N_2H_4BH_3$ apparently also play an indispensable role in their improved dehydrogenation properties. Finally, as the H-transfer mechanism proposed in MABs,[17] the presence of Li^+ in the current systems may also help to transfer H and release H_2 with the formation of LiH-intermediate.

The dehydrogenations of these compounds are exothermic; hence they cannot be directly rehydrogenated under H_2 pressure. The total observed H_2 release up to 400 °C from $LiN_2H_3BH_3$ and $LiN_2H_3BH_3 \cdot 2N_2H_4BH_3$ is 10.5 mass% and 11.5 mass%, respectively, which is less than their calculated H content (11.7 mass% and 14.0 mass%). This suggests that some H is still preserved in the spent fuel, consistent with the remaining NH and BH characteristic vibrations observed in IR spectra.[12] The XRD of the decomposition residues of $LiN_2H_3BH_3$ and $LiN_2H_3BH_3 \cdot 2N_2H_4BH_3$ revealed the formation of amorphous phases, which prevented direct determination of their structures. Nevertheless, the decomposition pathway of the HB molecule has been computationally well studied with boryl-hydrazine (BH_2NHNH_2) as the intermediate product after the loss of one H_2 per HB.[18] Identification of the crystal structures of $LiN_2H_3BH_3$ and $LiN_2H_3BH_3 \cdot 2N_2H_4BH_3$ will enable reaction path calculations of metal hydrazinoboranes and a direct comparison of the reaction enthalpies and barriers with HB, and thus promote further studies to achieve the possible reversibility in these materials.

$LiN_2H_3BH_3$ and $LiN_2H_3BH_3 \cdot 2N_2H_4BH_3$ are the first two examples of a potentially large class of metal hydrazinoboranes. The $[NH_2NHBH_3]^-$ is likely to bond with other metal elements to form a variety of corresponding hydrazinoboranes. For example, calcium hydrazinoborane was discovered after ball-milling a 1 : 2 CaH_2–HB mixture (Fig. S6†), and it also exhibited significantly promoted dehydrogenation compared to HB. In addition, in contrast to $[NH_2BH_3]^-$, the lone-pair electrons of the terminal N on $[NH_2NHBH_3]^-$ would also interact with the metal. Therefore, the bidentate nature of the $[NH_2NHBH_3]^-$ makes it serve as a bridging ligand and generate many interesting coordinations with metal cations. All of these should not only open a new avenue for hydrogen-storage materials, but also provide considerable new insight into the B–N chemistry.

Conclusions

We have successfully synthesized the first metal hydrazinoboranes, $LiN_2H_3BH_3$ and $LiN_2H_3BH_3 \cdot 2N_2H_4BH_3$. Their crystal structures have been determined using combined X-ray diffraction and molecular dynamics simulated annealing methods. The metal cation replaces one H on the middle N in the HB molecule, leading to the formation of $[NH_2NHBH_3]^-$. Metal hydrazinoboranes exhibit a much higher extent of dehydrogenation, minimized toxic gas release (*i.e.* NH_3, N_2H_4), and faster kinetics than pure HB. In particular, the extent and purity of H_2 released from $LiN_2H_3BH_3$ exceed even the best performance reported for hydrolysis of HB with catalysts. The electronic and structural changes from $N_2H_4BH_3$ to $[N_2H_3BH_3]^-$ are likely the main reasons for the observed improved hydrogen release process/kinetics for the metal hydrazinoboranes. Further studies need to be conducted in expanding the range of metals used in metal hydrazinoboranes, tuning the reactivity of B–H and/or N–H through inducing polar species such as strong electropositive cations or highly active anions, exploring the role of dopants or catalysts in controlling dehydrogenation, and understanding the dehydrogenation mechanism.

This work is partially supported by the DOE-EERE grant no. DE-EE0002978 (T.J.U.) and DOE-BES grant no. DE-FG02-08ER46522 (T.Y.).

Notes and references

1 F. Stephens, V. Pons and R. T. Baker, *Dalton Trans.*, 2007, 2613.
2 M. C. Denney, V. Pons, T. J. Hebden, M. Heinekey and K. I. Goldberg, *J. Am. Chem. Soc.*, 2006, **128**, 12048.
3 R. J. Keaton, J. M. Blacquiere and R. T. Baker, *J. Am. Chem. Soc.*, 2007, **129**, 1844–1845.
4 F. H. Stephens, R. T. Baker, M. H. Matus, D. J. Grant and D. A. Dixon, *Angew. Chem., Int. Ed.*, 2007, **46**, 746–749.
5 M. E. Bluhm, M. G. Bradley, R. Butterick, U. Kusari and L. G. Sneddon, *J. Am. Chem. Soc.*, 2006, **128**, 7748–7749.
6 G. Srinivas, J. Ford, W. Zhou, H. Wu, T. J. Udovic and T. Yildirim, *Chem.–Eur. J.*, 2011, **17**, 6043–6047.
7 A. D. Sutton, A. K. Burrell, D. A. Dixon, E. B. Garner, III, J. C. Gordon, T. Nakagawa, K. C. Ott, J. P. Robinson and M. Vasiliu, *Science*, 2011, **331**, 1426–1429.
8 V. J. Goubeau and E. Ricker, *Z. Anorg. Allg. Chem.*, 1961, **310**, 123–142.
9 R. Moury, G. Moussa, U. B. Demirci, J. Hannauer, S. Bernard, E. Petit, A. van der Lee and P. Miele, *Phys. Chem. Chem. Phys.*, 2012, **14**, 1768–1777.
10 J. Hannauer, O. Akdim, U. B. Demirci, C. Geantet, J. M. Herrmann, P. Miele and Q. Xu, *Energy Environ. Sci.*, 2011, **4**, 3355–3358.
11 S. Karahan, M. Zahmakiran and S. Ozkar, *Int. J. Hydrogen Energy*, 2011, **36**, 4958.
12 T. Hügle, M. F. Kühnel and D. Lentz, *J. Am. Chem. Soc.*, 2009, **131**, 7444–7446.
13 (*a*) Z. T. Xiong, C. K. Yong, G. T. Wu, P. Chen, W. Shaw, A. Karkamkar, T. Autrey, M. O. Jones, S. R. Johnson, P. P. Edwards and W. I. F. David, *Nat. Mater.*, 2008, **7**, 138; (*b*) H. Wu, W. Zhou and T. Yildirim, *J. Am. Chem. Soc.*, 2008, **130**, 14834–14839; (*c*) X. D. Kang, Z. Z. Fang, L. Y. Kong, H. M. Cheng, X. D. Yao, G. Q. Lu and P. Wang, *Adv. Mater.*, 2008, **20**, 2756; (*d*) H. V. K. Diyabalanage, T. Nakagawa, R. P. Shrestha, T. A. Semelsberger, B. L. Davis, B. L. Scott, A. K. Burrell, W. I. F. David, K. R. Ryan, M. O. Jones and P. P. Edwards, *J. Am. Chem. Soc.*, 2010, **132**, 11836; (*e*) H. Wu, W. Zhou, F. E. Pinkerton, M. S. Meyer, Q. R. Yao, S. Gadipelli, T. J. Udovic, T. Yildirim and J. J. Rush, *Chem. Commun.*, 2011, **47**, 4102; (*f*) K. J. Fijalkowski, R. V. Genova, Y. Filinchuk, A. Budzianowski, M. Derzsi, T. Jaroń, P. J. Leszczyński and W. Grochala, *Dalton Trans.*, 2011, **40**, 4407.
14 S. Mebs, S. Grabowsky, D. Forster, R. Kickbusch, M. Hartl, L. L. Daemen, W. Morgenroth, P. Luger, B. Paulus and D. Lentz, *J. Phys. Chem. A*, 2010, **114**, 10185–10196.
15 T. He, H. Wu, G. Wu, J. Wang, W. Zhou, Z. Xiong, J. Chen, T. Zhang and P. Chen, *Energy Environ. Sci.*, 2012, **5**, 5686–5689.
16 H. Wu, W. Zhou, F. E. Pinkerton, M. S. Meyer, G. Srinivas, T. Yildirim, T. J. Udovic and J. J. Rush, *J. Mater. Chem.*, 2010, **20**, 6550–6556.
17 (*a*) D. Y. Kim, N. J. Singh, H. M. Lee and K. S. Kim, *Chem.–Eur. J.*, 2009, **15**, 5598; (*b*) T. B. Lee and M. L. McKee, *Inorg. Chem.*, 2009, **48**, 7564.
18 V. S. Nguyen, S. Swinnen, M. H. Matus, M. T. Nguyen and D. A. Dixon, *Phys. Chem. Chem. Phys.*, 2009, **11**, 6339–6344.